Simple Model for Dynamic Heterogeneity in Glass-Forming Liquids

Rajib K. Pandit[*] and Horacio E. Castillo[†]

*Department of Physics and Astronomy and Nanoscale and Quantum Phenomena Institute, Ohio University,
Athens, Ohio 45701, USA*

Liquids near the glass transition exhibit dynamical heterogeneity, i.e., local relaxation rates fluctuate strongly over space and time. Here, we introduce a simple continuum model that allows for quantitative predictions for the correlators describing these fluctuations. We find remarkable agreement of the model predictions for the dynamic susceptibility $\chi_4(t)$ with numerical results for a binary hard-sphere liquid and for a Kob-Andersen Lennard-Jones mixture. Under this model, the lifetime τ_{ex} of the heterogeneities has little effect on the position $t = t_4 \sim \tau_\alpha$ of the peak of $\chi_4(t)$, but it controls the decay of $\chi_4(t)$ after the peak, and we show how to estimate it from this decay.

Introduction.—When cooled or compressed fast enough, most liquids will undergo a glass transition, where the characteristic timescale for relaxation, the α-relaxation time τ_α [1–3], grows smoothly but extremely rapidly. Together with the increase in relaxation time, *dynamical heterogeneity* emerges: relaxation becomes much slower in some regions than in others [2,4–6]. In this work we introduce a phenomenological model for dynamic heterogeneity which is directly based on this intuitive description and uses a local relaxation rate $\gamma(\vec{r}, t) \equiv 1/\tau_{\vec{r}}(t)$ as its basic variable. The model allows us to write the multipoint correlators measured in numerical simulations in terms of the two-point correlator $s(\vec{q}, t, t')$ of $\gamma(\vec{r}, t)$, which has a direct interpretation in terms of the size and lifetime of the heterogeneous regions. These quantities can provide a more direct connection between numerical simulation results and the results of experiments [4,6–8] on dynamical heterogeneity. More immediately, we show in this work that (i) numerical simulation data for two glass-forming systems [9,10] are consistent with predictions from the model; (ii) the model explains quantitatively and in a transparent way some of the general features [11] of the numerical results, and (iii) the model provides a new, simpler way to extract an estimate of the lifetime of the heterogeneities from numerical simulation data.

Probing relaxation in numerical simulations requires detecting changes in individual particle positions or orientations over a certain time interval of length t, i.e., measuring a two-time observable $C(t)$ [5]. For example, the overlap $C(t) = F_o(t)$ [9] gives the fraction of "slow particles," i.e., those particles that over the interval t have had displacements shorter than a certain distance a. Because of dynamic heterogeneity, the fraction of slow particles varies over space and time. This variation can be probed by measuring four-point functions such as the four-point structure factor $S_4(\vec{q}, t)$ [11–13], which is the Fourier-space correlation function of the *local* density of slow particles, or, equivalently, the structure factor of the slow particles (up to a trivial additive constant). The limit $\chi_4(t) = \lim_{q \to 0} S_4(\vec{q}, t)$ [9,11,13–15], called the *dynamic susceptibility*, captures contributions from dynamic heterogeneities of all spatial extents, and has been a central quantity in numerical studies of dynamical heterogeneity, where it has been often used to provide an overall measure of the degree of heterogeneity, or, in other words, of the intensity of the fluctuations. Although there have been some efforts to predict or interpret the time dependence of the four-point dynamic susceptibility $\chi_4(t)$, particularly for times up to the α relaxation time [14], much less is known about it for times $t > \tau_\alpha$, and about how the time evolution of $\chi_4(t)$ is connected with the time evolution of the heterogeneous regions.

Observables and data.—For simplicity, we consider only systems, such as supercooled liquids, where (i) the heterogeneity is dynamic, not static, and therefore all thermodynamic averages are translation invariant, and (ii) the dynamics is time-translation invariant (TTI), e.g., aging is not present. We also restrict ourselves to observables involving only one time interval from time 0 to time t. We probe the dynamics by using the microscopic overlap function $w_n(t) = \theta[a - |\vec{r}_n(t) - \vec{r}_n(0)|]$, where $\theta(x)$ is the Heaviside step function, $\vec{r}_n(t), n = 1, \ldots, N$ is the position of the nth particle at time t, and a is a characteristic distance that is larger than the typical amplitude of vibrational motion. We introduce the local relaxation function $C_{\vec{r}}(t)$,

$$C_{\vec{r}}(t) \equiv \rho^{-1} \sum_{n=1}^{N} w_n(t) \delta[\vec{r}_n(0) - \vec{r}], \quad \text{with} \quad \langle C_{\vec{r}}(t) \rangle = C(t),$$

$$(1)$$

where ρ is the average particle density, $\langle \cdots \rangle$ is an average over thermal fluctuations, and $C(t)$ is the global two-point

correlator, i.e., the average overlap $C(t) = F_o(t) \equiv N^{-1} \sum_{n=1}^{N} \langle w_n(t) \rangle$ [9]. Fluctuations are characterized by the four-point dynamic structure factor $S_4(\vec{q}, t)$ [11,12],

$$S_4(\vec{q}, t) \equiv \rho^2 N^{-1} \int d^d r\, e^{-i\vec{q}\cdot\vec{r}} \langle [C_{\vec{r}}(t) - C(t)][C_{\vec{0}}(t) - C(t)] \rangle \tag{2}$$

$$= N^{-1} \sum_{n,n'=1}^{N} \left\langle w_n(t) w_{n'}(t) e^{i\vec{q}\cdot[\vec{r}_n(0) - \vec{r}_{n'}(0)]} \right\rangle$$

$$- \delta_{\vec{q},0} N C^2(t). \tag{3}$$

Numerical results [16,17] are discussed for a 3D hard-sphere binary mixture (HARD) [9], and for a 3D Kob-Andersen Lennard-Jones binary mixture (KALJ) [10,18–20].

Continuum model for dynamic heterogeneity.—The model we introduce focuses on the α-relaxation regime, i.e., times t during the second step in the two-step relaxation. It is based on two assumptions, which we discuss below.

Motivation for Assumption 1.—Even though four-point functions were introduced to describe the collective phenomenon of dynamic heterogeneity, they capture much more than that. In Ref. [21] it was shown that at very long times t, the collective contributions to the four-point function $S_4(\vec{q}, t)$ are negligible compared to the single-particle, spatially uncorrelated, $\vec{q}$-independent contribution $S_4^{\mathrm{sp}}(\vec{q}, t) = \chi_4^{\mathrm{sp}}(t) \approx C(t) - C^2(t)$. To reproduce this behavior, we introduce the following:

Assumption 1.—The local relaxation function $C_{\vec{r}}(t)$ is the sum of two mutually independent random variables, the collective part $C_{\vec{r}}^{\mathrm{coll}}(t)$, and the single particle part $C_{\vec{r}}^{\mathrm{sp}}(t)$,

$$C_{\vec{r}}(t) = C_{\vec{r}}^{\mathrm{coll}}(t) + C_{\vec{r}}^{\mathrm{sp}}(t), \quad \text{with} \tag{4}$$

$$\langle C_{\vec{r}}^{\mathrm{coll}}(t) \rangle = C(t) \quad \text{and} \quad \langle C_{\vec{r}}^{\mathrm{sp}}(t) \rangle = 0. \tag{5}$$

We interpret all correlations between different particles as "collective," thus the single particle part $C_{\vec{r}}^{\mathrm{sp}}(t)$ is spatially uncorrelated at equal times,

$$G_4^{\mathrm{sp}}(\vec{r}, t) \equiv \rho \langle C_{\vec{r}}^{\mathrm{sp}}(t) C_{\vec{0}}^{\mathrm{sp}}(t) \rangle \propto \delta(\vec{r}), \text{ and } S_4^{\mathrm{sp}}(\vec{q}, t) = \chi_4^{\mathrm{sp}}(t). \tag{6}$$

Motivation for Assumption 2.—Dynamic heterogeneity has been described as involving relaxation times differing in different spatial regions [4,6,7], i.e., some regions being "fast" and others being "slow." Our model directly translates this intuitive description into quantitative predictions by defining a "local clock" $\phi_{\vec{r}}(t)$ (Fig. 1), which instead of counting in units of seconds, counts in units of the local relaxation time $\tau_{\vec{r}}(t)$,
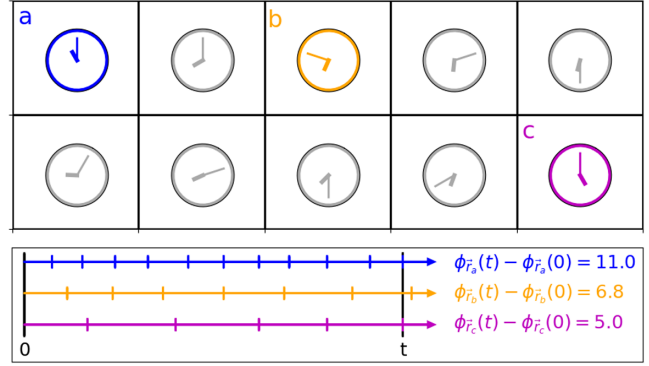
FIG. 1. *Converting the idea of space and time dependent relaxation times $\tau_{\vec{r}}(t)$ into the idea of a "local clock."* For each region in the system there is an individual local clock $\phi_{\vec{r}}(t)$ [Eq. (7)] that counts how many local relaxation times have elapsed up to time t. Each tic mark on a horizontal line represents one relaxation time. For example, of the three highlighted regions, a, b, and c, region c has relaxed the slowest, with $\Delta\phi_{\vec{r}_c}(t) = \phi_{\vec{r}_c}(t) - \phi_{\vec{r}_c}(0) = 5.0$ relaxation times elapsed between time 0 and time t. Regions a and b have relaxed generally faster, so the corresponding numbers of elapsed relaxation times between times 0 and t are larger, in this case $\Delta\phi_{\vec{r}_b}(t) = 6.8$ and $\Delta\phi_{\vec{r}_a}(t) = 11.0$.

$$\phi_{\vec{r}}(t) \equiv \int^t dt' / \tau_{\vec{r}}(t'). \tag{7}$$

Thus, $\Delta\phi_{\vec{r}}(t) \equiv \phi_{\vec{r}}(t) - \phi_{\vec{r}}(0)$ represents the number of relaxation times elapsed between times 0 and t in the region around $\vec{r}$ (Fig. 1). Naively, one could expect $C_{\vec{r}}^{\mathrm{coll}}(t)$ to depend only on $\Delta\phi_{\vec{r}}(t)$, i.e., $C_{\vec{r}}^{\mathrm{coll}}(t) = \mathcal{C}[\Delta\phi_{\vec{r}}(t)]$ [22–24]. Here, $\mathcal{C}(x)$ does not fluctuate, it is a fixed monotonous decreasing function, with $\mathcal{C}(1) = e^{-1} \mathcal{C}(0)$, that represents the shape of the local relaxation function, for example, $\mathcal{C}(x) = f_0 \exp(-x)$ for simple exponential relaxation. This ansatz, however, does not reproduce $S_4(\vec{q}, t)$, because spatial density fluctuations in the initial state of the system provide two $\vec{q}$-dependent contributions [21] to $S_4(\vec{q}, t)$. One is $S_4^{\mathrm{st}}(\vec{q}, t) = C^2(t)S(\vec{q})$ (for $q \neq 0$), where $S(\vec{q})$ is the static structure factor; the other, S_4^{mc} [16] was neglected in the case of $\chi_4(t) = \lim_{q\to 0} S_4(\vec{q}, t)$. This motivates multiplying $\mathcal{C}[\Delta\phi_{\vec{r}}(t)]$ by the initial local particle density $\rho(\vec{r}, 0)$, which leads to

Assumption 2.—The collective contribution is

$$C_{\vec{r}}^{\mathrm{coll}}(t) = \rho^{-1} \rho(\vec{r}, 0) \mathcal{C}[\phi_{\vec{r}}(t) - \phi_{\vec{r}}(0)], \tag{8}$$

$$\text{where } \partial\phi_{\vec{r}}(t)/\partial t \equiv 1/\tau_{\vec{r}}(t) = \gamma(\vec{r}, t) \tag{9}$$

is the local relaxation rate. For simplicity, we assume that $\rho(\vec{r}, t_1)$ and $\phi_{\vec{r'}}(t_2)$ are mutually independent random variables, for arbitrary positions $\vec{r}$, $\vec{r'}$, and times t_1, t_2, and that they are smooth and slowly varying in space and time.

Motivation for the definition of $\tau_{\rm ex}$.—The exchange time $\tau_{\rm ex}$ has been defined as the characteristic time for a "fast" region becoming "slow" or vice versa [4,6,7]. This translates directly into defining it as the characteristic time for the autocorrelation function of the relaxation rate $\gamma(\vec{r},t) = 1/\tau_{\vec{r}}(t)$.

Definition of the exchange time $\tau_{\rm ex}$.—

$$\tau_{\rm ex} \equiv \frac{\int_0^\infty t \chi_2^\phi(t)\,dt}{\int_0^\infty \chi_2^\phi(t)\,dt}, \quad \text{where } \chi_2^\phi(t) \equiv \lim_{q\to 0} s(\vec{q},t), \quad (10)$$

and

$$s(\vec{q},t) \equiv V^{-1} \int d^d r\, e^{-i\vec{q}\cdot\vec{r}} \langle \delta\gamma(\vec{r},t)\delta\gamma(\vec{0},0)\rangle. \quad (11)$$

Here, $\chi_2^\phi(t)$ and $s(\vec{q},t)$ are two-point functions of the fluctuations $\delta\gamma(\vec{r},t) \equiv \gamma(\vec{r},t) - \langle\gamma(\vec{r},t)\rangle$ of the relaxation rate. The limit $q\to 0$ in Eq. (10) includes fluctuations at all spatial length scales, as in the definition of $\chi_4(t)$ [9,11,13–15].

Results: Prediction for the dynamic susceptibility $\chi_4(t)$.—By Taylor expanding Eq. (8) up to quadratic order in $\delta\gamma$, Assumptions 1 and 2 lead to

$$\mathcal{C}'(t/\tau) \approx \tau\dot{C}(t), \quad \text{where } C(\tau) = e^{-1}, \quad \text{and} \quad (12)$$

$$\chi_4(t) \equiv \lim_{q\to 0} S_4(\vec{q},t) = \dot{C}^2(t)\tilde{\chi}_4^\phi(t) + \chi_{4,b}^{(0)}(t), \quad \text{with} \quad (13)$$

$$\chi_{4,b}^{(0)}(t) \equiv C(t) + [N^{-1}\langle(\delta N)^2\rangle - 1]C^2(t) \quad (14)$$

representing a background due to single particle and initial density fluctuations.

Equation (13) is the main result of this work. The factor $\dot{C}^2(t)$ comes directly from the linear term in the Taylor expansion, and its presence is unavoidable for any ansatz that contains a factor like $\mathcal{C}[\phi_{\vec{r}}(t) - \phi_{\vec{r}}(0)]$ that attempts to represent the effects of fluctuating local relaxation rates. The factor $\tilde{\chi}_4^\phi(t)$ [25] is predicted to be a positive monotonously increasing function of t, which has no special feature for $t \sim \tau_\alpha$ (Fig. 2). Initially, $\chi_4(t)$ grows rapidly due to the rapid growth of $\tilde{\chi}_4^\phi(t)$, but this growth gets cut off by the sharp decrease of $\dot{C}^2(t)$ near $t \sim \tau_\alpha$, corresponding to the fact that τ_α is the characteristic time for the decay of $C(t)$. This leads to $\chi_4(t)$ having its peak for $t \sim \tau_\alpha$ [11,14], even if the exchange time is much longer [26]. Another way of looking at this is to rewrite $\dot{C}^2(t)\tilde{\chi}_4^\phi(t) = [t^2\dot{C}^2(t)][t^{-2}\tilde{\chi}_4^\phi(t)]$, where $t^{-2}\tilde{\chi}_4^\phi(t)$ is still featureless for $t \sim \tau_\alpha$ (Fig. 2), but $t^2\dot{C}^2(t)$ has a peak at $t \sim \tau_\alpha$, which leads to the peak in $\chi_4(t)$. $\tilde{\chi}_4^\phi(t)$ controls the height of the peak of $\chi_4(t)$, and provides an overall measure of the heterogeneity, because it is approximately proportional to the mean quadratic drift $\langle[\Delta\phi_{\vec{r}}(t) - \langle\Delta\phi_{\vec{r}}(t)\rangle]^2\rangle = \langle[\int_0^t \delta\gamma(\vec{r},t)]^2\rangle = \int_0^t dt'' \int_0^t dt'\chi_2^\phi(t''-t')$ of the local clocks,
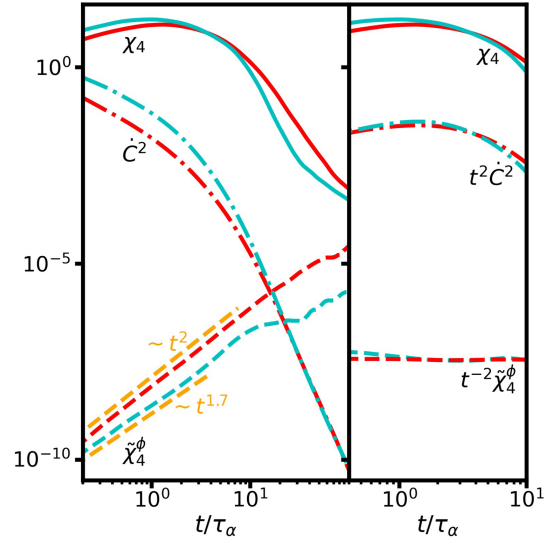

FIG. 2. Numerical results [17] for KALJ (cyan) and HARD (red). Left panel: $\chi_4(t)$ for KALJ for $T = 0.50$ and for HARD at $\varphi = 0.58$, $10^6 \dot{C}^2(t)$ for KALJ at $T = 0.50$ and $10^{10}\dot{C}^2(t)$ for HARD at $\varphi = 0.58$, $10^{-21}\tilde{\chi}_4^\phi(t)$ [25] for HARD at $\varphi = 0.58$, and $10^{-17}\tilde{\chi}_4^\phi(t)$ for KALJ at $T = 0.50$. $\tilde{\chi}_4^\phi(t)$ is extracted from the data by $\tilde{\chi}_4^\phi(t) = [\chi_4(t) - \chi_{4,b}^{(0)}(t)]\dot{C}^{-2}(t)$. The yellow dashed lines represent a $\propto t^2$ time dependence [frozen heterogeneity approximation for $\tilde{\chi}_4^\phi(t)$], and a $\propto t^{1.7}$ time dependence. Right panel: $\chi_4(t)$ for KALJ at $T = 0.50$ and for HARD at $\varphi = 0.58$, $t^2\dot{C}^2(t)$ for KALJ at $T = 0.50$ and for HARD at $\varphi = 0.58$, $10^{-10}t^{-2}\tilde{\chi}_4^\phi(t)$ for HARD at $\varphi = 0.58$ and for KALJ at $T = 0.50$.

$$\tilde{\chi}_4^\phi(t) \equiv \rho\tau^2 \int_0^t dt'' \int_0^t dt'\tilde{\chi}_2^\phi(t''-t'), \quad \text{with} \quad (15)$$

$$\tilde{\chi}_2^\phi(t) \equiv \chi_2^\phi(t) + \lim_{q\to 0}\rho^{-1}\{[S_c(\cdot)-1]\circ s(\cdot,t)\}(\vec{q}), \quad (16)$$

where $S_c(\vec{q}) \equiv [S(\vec{q}) - \rho\delta_{\vec{q},\vec{0}}]$ is the connected part of the static structure factor and $f \circ g$ denotes a convolution. In fact, in most cases, $\tilde{\chi}_2^\phi(t) \approx \chi_2^\phi(t)$ [25].

Results: Upper bound for $\chi_4(t)$ *and frozen heterogeneity approximation.*—Equations (13) and (15) imply there is an upper bound $\chi_{4,\rm fh}(t)$ for $\chi_4(t)$,

$$\chi_4(t) \le \chi_{4,\rm fh}(t) \equiv \tilde{a}_\phi t^2\dot{C}^2(t) + \chi_{4,b}^{(0)}(t), \quad \text{with} \quad (17)$$

$$\tilde{a}_\phi \equiv \rho\tau^2\tilde{\chi}_{2,M} \quad \text{and} \quad \tilde{\chi}_{2,M} \equiv \sup_t \tilde{\chi}_2^\phi(t) < \infty, \quad (18)$$

where the parameter $\tilde{a}_\phi$ [25] represents the overall strength of the heterogeneity.

For times $\tau_\alpha \lesssim t \ll \tau_{\rm ex}$, most slow (fast) regions will stay slow (fast), so that each of their local clock drifts $\int_0^t \delta\gamma(\vec{r},t)$ will grow linearly with time. Thus, for $\tau_\alpha \lesssim t \ll \tau_{\rm ex}$, $\tilde{\chi}_4^\phi(t) \propto \langle(\text{local clock drift})^2\rangle \propto t^2$. (Figure 2 shows that this regime can be found for HARD but not for KALJ.)
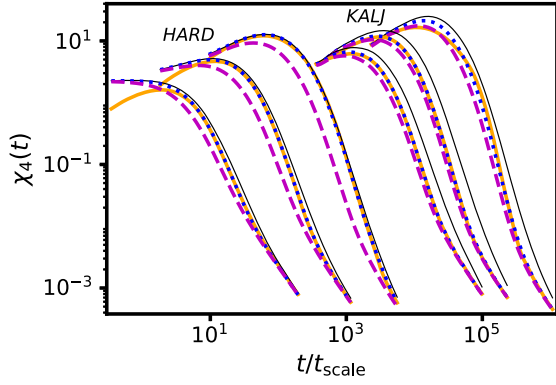
FIG. 3. Comparison of our model's predictions for $\chi_4(t)$, Eqs. (13)–(15), with numerical simulation results [17] (orange full lines) for HARD for packing fractions $\varphi = 0.55$, 0.57, 0.58 (left side, left to right) and KALJ for temperatures $T = 0.60$, 0.55, 0.50 (right side, left to right). t_{scale} is 1 for HARD and 0.005 for KALJ. Model predictions are shown for (i) the frozen heterogeneity approximation $\chi_4(t) = \chi_{4,\text{fh}}(t)$ (black thin lines); (ii) $\tilde{\chi}_2^\phi(t) = \tilde{\chi}_2^\phi(0)e^{-t/\tilde{\tau}_{\text{ex}}}$ with $\tilde{\tau}_{\text{ex}} = \tau_\alpha$ [25] (magenta dashed lines); and (iii) $\tilde{\chi}_2^\phi(t) = \tilde{\chi}_2^\phi(0)e^{-t/\tilde{\tau}_{\text{ex}}}$ with $\tilde{\tau}_{\text{ex}}$ chosen by fitting the data with Eq. (19) (blue dotted lines).

Equivalently, for $0 < t' < t \ll \tau_{\text{ex}}$, $\tilde{\chi}_2^\phi(t') \approx \tilde{\chi}_{2,M}$ [25]. Thus, Eq. (17) becomes an approximate equality, $\chi_4(t) \approx \chi_{4,\text{fh}}(t)$. We refer to this as the *frozen heterogeneity approximation*. In this approximation, the time dependence of the dynamic susceptibility $\chi_4(t)$ is given by an explicit expression in terms of independently measured quantities —$C(t)$ and $\langle(\delta N)^2\rangle$—plus a single numerical constant $\tilde{a}_\phi$.

By contrast, for $t \gtrsim \tau_{\text{ex}}$ the inequality in Eq. (17) becomes strict. For $t \gg \tau_{\text{ex}}$, a given region will pass through periods in which it is slow and periods in which it is fast, so local drifts will alternate between positive and negative signs, and $\tilde{\chi}_4^\phi(t) \propto \langle(\text{local clock drift})^2\rangle \ll (\text{const})t^2$. In particular, if $\tilde{\chi}_2^\phi(t)$ decays like $t^{-1-\delta}(\delta > 0)$ or faster, then $\tilde{\chi}_4^\phi(t) \propto t \ll t^2$.

Figure 3 shows a comparison of our model's predictions for $\chi_4(t)$ with numerical results [17] for HARD and KALJ. To explore the effects of the exchange time on the results, we choose the simple parametrization $\tilde{\chi}_2^\phi(t) = \tilde{\chi}_2^\phi(0)e^{-t/\tilde{\tau}_{\text{ex}}}$, which by Eq. (15) gives

$$\tilde{\chi}_4^\phi(t) = \tilde{a}_\phi\{2\tilde{\tau}_{\text{ex}}^2[\exp(-t/\tilde{\tau}_{\text{ex}}) - 1 + t/\tilde{\tau}_{\text{ex}}]\}. \quad (19)$$

There is a narrow band of possible results of the model between the cases of frozen heterogeneity [$\tilde{\tau}_{\text{ex}} = \infty$, $\chi_4(t) = \chi_{4,\text{fh}}(t)$] and of $\tilde{\tau}_{\text{ex}} = \tau_\alpha$. The numerical results fall within that range for $t \gtrsim \tau_\alpha$ for HARD at $\varphi = 0.55$, 0.57 and for $t \gtrsim 0.1\tau_\alpha$ for all other cases [16]. For HARD they approach the frozen heterogeneity upper bound $\chi_{4,\text{fh}}(t)$ as the packing fraction increases. For KALJ, they are closer to the $\tau_{\text{ex}} = \tau_\alpha$ results. In fact, remarkable agreement can be
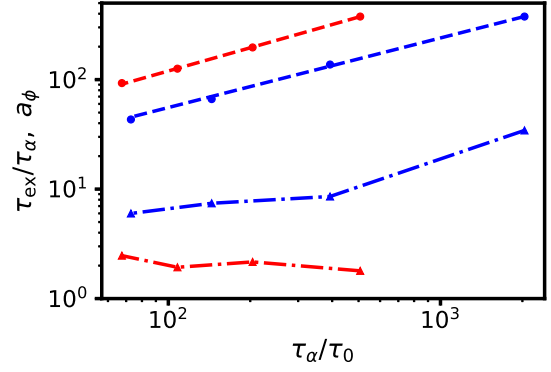

FIG. 4. Ratio $Q = \tau_{\text{ex}}/\tau_\alpha$ (triangles) and heterogeneity strength parameter a_ϕ (circles), vs rescaled relaxation time τ_α/τ_0 ([10]), for HARD (blue) at $\varphi = 0.55$, 0.56, 0.57, 0.58 and KALJ (red) at $T = 0.70$, 0.65, 0.60, 0.55. The dashed lines are power law fits for a_ϕ.

obtained if the form in Eq. (19) is used, with $\tilde{\tau}_{\text{ex}}$ as a fitting parameter. (For KALJ at $T = 0.50$, the data are too noisy to judge on goodness of fit.)

Results: Exchange time τ_{ex}.—Figure 4 shows initial estimates of the memory parameter $Q \equiv \tau_{\text{ex}}/\tau_\alpha$ [7] and the heterogeneity strength parameter a_ϕ, obtained under the assumption that $\chi_2^\phi(t) = \chi_2^\phi(0)e^{-t/\tau_{\text{ex}}}$, which corresponds to $\chi_4(t) = \dot{C}^2(t)a_\phi\{2\tau_{\text{ex}}^2[\exp(-t/\tau_{\text{ex}}) - 1 + t/\tau_{\text{ex}}]\} + \chi_{4,b}(t)$ [16]. For KALJ $Q \sim 2$ and it seems not to vary strongly with τ_α [26], but for HARD, Q increases from ~ 5 to $\gtrsim 30$ as the glass transition is approached. For both models, $a_\phi \sim \tau_\alpha^p$, with $p_{\text{HARD}} \approx 0.64$ and $p_{\text{KALJ}} \approx 0.70$.

Summary.—We have introduced a simple phenomenological model for dynamic heterogeneity in glass-forming materials. This model translates into quantitative predictions the intuitive description of dynamic heterogeneities as local fluctuations in the relaxation rate, and additionally takes into account contributions due to local particle density fluctuations and to single-particle, noncollective behavior.

The model provides expressions for computing four-point functions—such as Eqs. (13)–(16)—requiring only one- and two-point quantities—like ρ, $S(\vec{q})$, $C(t)$, and the relaxation rate two-point correlation function $s(\vec{q}, t)$—that are much easier to interpret than four-point functions. Crucially, Eq. (13) shows that $\chi_4(t)$ having a peak at $t \sim \tau_\alpha$ is due to $\dot{C}^2(t)$ having its characteristic time at $t \sim \tau_\alpha$, even though $\tilde{\chi}_4^\phi(t)$ is the factor that most directly encodes the time dependence of relaxation rate fluctuations. This explains why the lifetime of the dynamic heterogeneities has a weak effect on the location $t = t_4 \sim \tau_\alpha$ of the peak of $\chi_4(t)$.

Given a single parameter $\tilde{a}_\phi$ encoding the overall strength of the relaxation rate fluctuations, the model predicts an upper bound $\chi_{4,\text{fh}}(t)$ for the dynamic susceptibility $\chi_4(t)$, corresponding to the limit of frozen

heterogeneity, $\tilde{\tau}_{\mathrm{ex}} = \infty$. If, additionally, it is assumed that the two-point susceptibility decays exponentially, $\tilde{\chi}_2^\phi(t) = \tilde{\chi}_2^\phi(0)e^{-t/\tilde{\tau}_{\mathrm{ex}}}$, very good agreement is obtained with numerical data by fitting with the two parameters $\tilde{a}_\phi$, $\tilde{\tau}_{\mathrm{ex}}$. The dependence of $\chi_4(t)$ on $\tilde{\tau}_{\mathrm{ex}}$ is relatively weak, and all numerical data fall in the narrow interval between the $\tilde{\tau}_{\mathrm{ex}} = \tau_\alpha$ prediction and the frozen heterogeneity $\tilde{\tau}_{\mathrm{ex}} = \infty$, $\chi_4(t) = \chi_{4,\mathrm{fh}}(t)$ prediction.

Information about the time evolution of the heterogeneities can be found most clearly in the time evolution of $\chi_4(t)$ *after* its peak. Roughly speaking, $\tau_{\mathrm{ex}} = \infty$ makes the heterogeneities maximally persistent, which maximizes the strength of the heterogeneity, i.e., $\chi_4(t) \approx \chi_{4,\mathrm{fh}}(t)$, but the shorter τ_{ex} is, the faster the heterogeneous relaxation rates return to the mean, and the more $\chi_4(t)$ differs from $\chi_{4,\mathrm{fh}}(t)$ for times $t \gtrsim \tau_{\mathrm{ex}}$. Estimating $Q = \tau_{\mathrm{ex}}/\tau_\alpha$ from $\chi_4(t)$ shows that $Q_{\mathrm{KALJ}} \sim 2$ independently of τ_α [26], but Q_{HARD} grows strongly with τ_α. (We believe this to be the first measurement of Q or τ_{ex} for a hard sphere model.) These results are consistent with the fact that for HARD at higher packing fraction (but not for KALJ), there is a time regime $\tau_\alpha \lesssim t \ll \tau_{\mathrm{ex}}$ where the frozen heterogeneity approximation holds, i.e., $\tilde{\chi}_4^\phi(t) \sim t^2$ (Fig. 2) and $\chi_4(t) \approx \chi_{4,\mathrm{fh}}(t)$ (Fig. 3).

Finally, the model introduces $s(\vec{q}, t)$, which quantifies more directly the spatial and temporal correlations of the local relaxation rate. Results for this quantity, plus discussions of non-TTI dynamics, more general overlap functions $w_n(t)$, four-point functions with general time arguments, and connections to experimentally measured correlators [4,6–8], will be reported elsewhere [27,28].

[*]Present address: Exact Sciences, Redwood City, California 94063, USA.
[†]castillh@ohio.edu

[1] E. Donth, *The Glass Transition* (Springer-Verlag, Berlin, 2001).
[2] C. A. Angell, K. L. Ngai, G. B. McKenna, P. F. McMillan, and S. W. Martin, J. Appl. Phys. **88**, 3113 (2000).
[3] P. G. Debenedetti and H. Stillinger Frank, Nature (London) **410**, 259 (2001).
[4] M. D. Ediger, Annu. Rev. Phys. Chem. **51**, 99 (2000).
[5] *Dynamical Heterogeneities in Glasses, Colloids, and Granular Media*, edited by L. Berthier, G. Biroli, J.-P. Bouchaud, L. Cipelletti, and W. van Saarloos (Oxford University Press, New York, 2011).
[6] H. Sillescu, J. Non-Cryst. Solids **243**, 81 (1999).
[7] R. Richert, Proc. Natl. Acad. Sci. U.S.A. **112**, 4841 (2015).
[8] K. Paeng, H. Park, D. T. Hoang, and L. J. Kaufman, Proc. Natl. Acad. Sci. U.S.A. **112**, 4952 (2015).
[9] E. Flenner, M. Zhang, and G. Szamel, Phys. Rev. E **83**, 051501 (2011).
[10] E. Flenner, H. Staley, and G. Szamel, Phys. Rev. Lett. **112**, 097801 (2014).
[11] N. Lačević, F. W. Starr, T. B. Schrøder, and S. C. Glotzer, J. Chem. Phys. **119**, 7372 (2003).
[12] C. Dasgupta, A. V. Indrani, S. Ramaswamy, and M. K. Phani, Europhys. Lett. **15**, 307 (1991).
[13] L. Berthier and G. Biroli, Rev. Mod. Phys. **83**, 587 (2011).
[14] C. Toninelli, M. Wyart, L. Berthier, G. Biroli, and J.-P. Bouchaud, Phys. Rev. E **71**, 041505 (2005).
[15] A. Parsaeian and H. E. Castillo, Phys. Rev. E **78**, 060105(R) (2008).
[16] See Supplemental Material at http://link.aps.org/supplemental/10.1103/PhysRevLett.131.218202 for additional details.
[17] Ohio Supercomputer Center, Ohio Supercomputer Center, http://osc.edu/ark:/19495/f5s1ph73 (1987).
[18] W. Kob and H. C. Andersen, Phys. Rev. Lett. **73**, 1376 (1994).
[19] W. Kob and H. C. Andersen, Phys. Rev. E **51**, 4626 (1995).
[20] W. Kob and H. C. Andersen, Phys. Rev. E **52**, 4134 (1995).
[21] R. K. Pandit, E. Flenner, and H. E. Castillo, Phys. Rev. E **105**, 014605 (2022).
[22] G. A. Mavimbela, A. Parsaeian, and H. E. Castillo, arXiv:1210.1249.
[23] G. A. Mavimbela, A. Parsaeian, and H. E. Castillo, AIP Adv. **9**, 015210 (2019).
[24] R. K. Pandit, Local fluctuations in the relaxation rate in glassy systems, Ph.D. thesis, Ohio University, 2019, https://etd.ohiolink.edu/acprod/odb_etd/ws/send_file/send?accession=ohiou1542389277929449&disposition=inline.
[25] The tilde symbol ˜ identifies five quantities, i.e., $\tilde{\chi}_4^\phi(t)$, $\tilde{\chi}_2^\phi(t)$, $\tilde{\chi}_{2,M}$, $\tilde{\tau}_{\mathrm{ex}}$, and $\tilde{a}_\phi$, that mostly quantify relaxation rate fluctuations but contain a small correction from density fluctuations. (See Supplemental Material for additional details.)
[26] K. Kim and S. Saito, J. Chem. Phys. **138**, 12A506 (2013).
[27] R. K. Pandit and H. E. Castillo (to be published).
[28] H. E. Castillo and R. K. Pandit (to be published).